

# Suppression of energy-relaxation-induced decoherence in $\Lambda$ -type three-level SQUID flux qubits: A dark-state approach

Zhongyuan Zhou,<sup>1,2</sup> Shih-I Chu,<sup>1</sup> and Siyuan Han<sup>2</sup>

<sup>1</sup>*Department of Chemistry, University of Kansas, Lawrence, Kansas 66045, USA*

<sup>2</sup>*Department of Physics and Astronomy, University of Kansas, Lawrence, Kansas 66045, USA*

(Received 5 March 2004; revised manuscript received 9 June 2004; published 23 September 2004)

We report a theoretical investigation of decoherence induced by energy relaxation of the auxiliary level in the  $\Lambda$ -type three-level SQUID flux qubits. We show that the energy-relaxation-induced decoherence in this particular case is proportional to the average population of the auxiliary level and thus can be effectively suppressed by the use of a dark-state approach in which the auxiliary level is unpopulated. We demonstrate through bit-flip operation that the dark state can be realized by means of the stimulated Raman adiabatic passage (STIRAP). An extension of the dark-state scheme to create any superposition state is straightforward.

DOI: 10.1103/PhysRevB.70.094513

PACS number(s): 03.67.Lx, 85.25.Dq, 89.70.+c

The elementary unit of a quantum computer is a qubit which, in the simplest case, is a two-level quantum system. A qualified qubit requires quantum coherence of the qubit states be maintained during the quantum computation and communication since these operations are performed via quantum superposition states and entanglement states of the qubit.<sup>1,2</sup> In an actual qubit, the coherence can be destroyed by decoherence such as dephasing and energy relaxation.<sup>2,3</sup> In superconducting qubits based on Josephson junctions, several main sources of dephasing, such as background charge fluctuation, bias flux fluctuation, and critical current fluctuation, have been recently discussed.<sup>4-7</sup> The results indicate that the decoherence due to these mechanisms is not the limiting factor for superconducting flux qubits.<sup>4,5</sup> Energy relaxation which results in the spontaneous decay of the qubit states is due to and proportional to finite damping in the qubit. For a qubit with two long-lifetime computational levels, such as the lowest level in each of the double-well potentials of a superconducting quantum interference device (SQUID), decoherence induced by energy relaxation does not pose a serious problem as long as the junction's effective resistance is reasonably high. For instance, for a rf SQUID qubit with a moderate damping resistance  $R=10\text{ M}\Omega$  the energy relaxation time  $T_1$  could exceed 10 ms.

For a physical qubit with more than two levels, such as the SQUID flux qubit, coherent state manipulation may also suffer from other sources of decoherence, such as the coupling of the qubit's two-computational states to its noncomputational states.<sup>8,9</sup> For this kind of qubit, even in the absence of energy relaxation and dephasing, the qubit could have significant intrinsic errors elicited by leakage to the noncomputational states and strong field effect when the qubit states are manipulated by resonant microwave pulses.<sup>9</sup> To circumvent these shortcomings of the two-level qubits (2LQ) in a multi-level system, we proposed the  $\Lambda$ -type three-level SQUID flux qubits (3LQ).<sup>9</sup> In the 3LQ, an auxiliary level  $|a\rangle$  is utilized to create a stronger effective coupling between the computational levels  $|0\rangle$  and  $|1\rangle$  of the qubit. In comparison with the 2LQ, the 3LQ is

much faster and much less susceptible to the strong field induced multiphoton process which is one of the main mechanisms of the gate errors of the 2LQ. Due to these advantages, the 3LQ has become a promising candidate in the quantum computation and communication based on SQUID qubits.<sup>10,11</sup>

However, in a real 3LQ, using the auxiliary level with finite population results in additional decoherence associated with dephasing and energy relaxation due to damping. For a SQUID flux qubit, because the dephasing caused by the external fluctuations is small,<sup>4,5</sup> the characteristic time of dephasing  $T_2$  is about two times of that of energy relaxation  $T_1$ .<sup>12</sup> Thus the energy relaxation is a main source of the decoherence for the SQUID flux qubits. If no population resides on the auxiliary level at any time during the state manipulation (a dark auxiliary state), the population transfer will not be affected by spontaneous decay from the auxiliary level.<sup>13,14</sup>

For a  $\Lambda$ -type three-level system without dissipation, the dark state  $|D\rangle = \cos\theta(t)|0\rangle - \sin\theta(t)|1\rangle$  is an eigenstate of the system, here  $\tan\theta(t) \equiv \Omega_0(t)/\Omega_1(t)$  is the ratio of the two Rabi frequencies for the  $|i=0,1\rangle \leftrightarrow |a\rangle$  transition.<sup>15-18</sup> Adiabatic population transfer between  $|0\rangle$  and  $|1\rangle$  can be realized by using two partially overlapping counterintuitive pulses. This scheme of population transfer, which is known as stimulated Raman adiabatic passage (STIRAP), has been studied extensively both theoretically<sup>16,18,19</sup> and experimentally<sup>20,21</sup> since it was first observed.<sup>22</sup> For a dissipative  $\Lambda$ -type three-level system, nonadiabatic population transfer has been recently studied analytically for special pulse shapes.<sup>13,14</sup> The population transfer depends strongly on the decay rate of the auxiliary level and thus the loss of population is large when the auxiliary level is significantly populated during the population transfer.

However, there are significant differences between the SQUID flux qubit and an ideal  $\Lambda$ -type three-level system: (i) The SQUID flux qubit has many additional levels which are not well separated (in energy) from the three levels utilized for coherent population transfer; (ii) the coupling between

the computational levels and noncomputational levels is relatively strong, particularly the coupling between the auxiliary level and the noncomputational levels; (iii) the excited states of the flux qubit have relatively shorter lifetimes. Therefore, it is rather difficult to quantitatively evaluate the performance of the flux qubit in terms of the analytical results obtained from the ideal  $\Lambda$ -type three-level system and thus numerical studies are necessary. In this paper, we investigate quantitatively, through an accurate numerical calculation of the population evolution of the multi-level SQUID flux qubit with realistic device parameters including finite damping, the effect of energy relaxation on the decoherence in 3LQ as a function of population on the level  $|a\rangle$  and the method to reduce the population of the auxiliary level during the bit-flip operation. In particular, our study does not make the rotating wave and three-level approximations. We show that decoherence is proportional to the average population of the auxiliary level and therefore can be effectively suppressed with the use of a dark-state approach.<sup>13–15,23</sup> We demonstrate that a dark auxiliary state in the 3LQ can also be achieved by means of STIRAP.

A SQUID consists of a superconducting loop of inductance  $L$  interrupted by a Josephson tunnel junction, which is characterized by its critical current  $I_c$ , shunt capacitance  $C$ , and shunt resistance  $R$ . The Hamiltonian of a dissipationless ( $R \rightarrow \infty$ ) SQUID is

$$H_0(x) = p_x^2/2m + U(x), \quad (1)$$

where,  $x = \Phi/\Phi_0$ ,  $p_x = -i\hbar\partial/\partial x$ ,  $\Phi$  is the total magnetic flux enclosed in the SQUID loop,  $\Phi_0 \equiv h/2e$  is the flux quantum, and  $m = C\Phi_0^2$ . The potential energy is

$$U(x) = \frac{1}{2}m\omega_{LC}^2(x - x_e)^2 - \frac{1}{4\pi^2}m\omega_{LC}^2\beta_L \cos 2\pi x. \quad (2)$$

The geometric shape of the potential is determined completely by the dimensionless parameters  $\beta_L \equiv 2\pi L I_c / \Phi_0$  and  $x_e \equiv \Phi_e / \Phi_0$ , where  $\Phi_e$  is the flux applied to the SQUID. If  $\hbar\omega_{LC}$  is used as the unit of energy, where  $\omega_{LC} \equiv 1/\sqrt{LC}$  is characteristic frequency of the qubit, the eigenstates of the SQUID only depend on two independent parameters,  $\beta_L$  and  $Z_0 \equiv \sqrt{L/C}$  (the characteristic impedance). A SQUID with  $\beta_L = 1.20$ ,  $Z_0 = 50 \Omega$ ,  $\omega_{LC} = 5 \times 10^{11}$  rad/s, and  $x_e = 0.499$ , is used throughout this work.<sup>9</sup>

To study population evolution, we expand a time-dependent wave function in eigenfunctions of the field-free Hamiltonian  $H_0(x)$ . The expansion coefficient vector,  $\mathbf{C}(\tau) = \{c_n(\tau)\}$  ( $n = 1, 2, \dots, N$ , with  $N$  the number of eigenstates in the expansion), is governed by the time-dependent Schrödinger equation,

$$i \frac{d}{d\tau} \mathbf{C}(\tau) = H(\tau) \mathbf{C}(\tau), \quad (3)$$

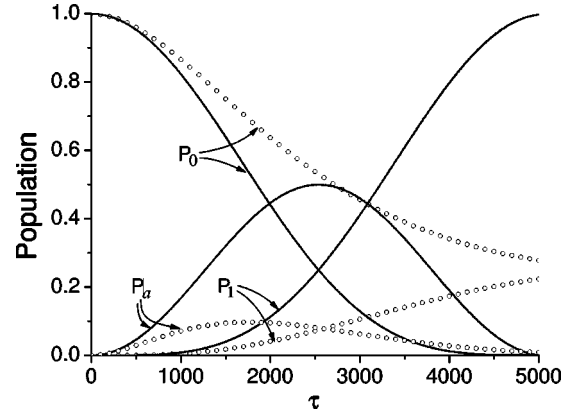


FIG. 1. The evolution of populations on the computational and auxiliary levels of the 3LQ using two overlapping rectangular microwaves. The solid lines are the populations for  $\gamma_a = 0$  and the open circles are the populations for  $\gamma_a = 1.86 \times 10^{-3}$ . The pulse amplitudes are  $A_0 = 2 \times 10^{-4}$  and  $A_1 = 1.48 \times 10^{-4}$ .

$$H_{nn'}(\tau) = \varepsilon_n \delta_{nn'} + \frac{m\omega_{LC}x_\mu(\tau)}{\hbar} \left[ x_{nn'} + \left( \frac{1}{2}x_\mu(\tau) - x_e \right) \delta_{nn'} \right]. \quad (4)$$

Here,  $\tau \equiv \omega_{LC}t$  is reduced time,  $\varepsilon_n = E_n/\hbar\omega_{LC}$  is reduced eigenenergy, and  $x_{nn'} = \langle n|x|n' \rangle$  is the dipole matrix element. The total magnetic flux coupled to the qubit from the microwave field  $x_\mu(\tau)$  (normalized to  $\Phi_0$ ) is a superposition of the flux from two microwave pulses:  $x_\mu(\tau) = \sum_{i=0,1} x_{\mu i}(\tau)$  with  $x_{\mu i} = A_i f_i(\tau) \sin \omega_i \tau$ , and  $\omega_i$ ,  $A_i$ , and  $0 \leq f_i(\tau) \leq 1$  are the angular frequency (normalized to  $\omega_{LC}$ ), amplitude, and dimensionless pulse shape function of the  $i$ th pulse which is finite for  $0 \leq \tau \leq \tau_i$  and is zero otherwise. For resonant pulses, one has  $\omega_i = \varepsilon_a - \varepsilon_i$  for  $i = 0, 1$ . The coefficient vector and therefore the population  $P_n = |c_n(\tau)|^2$  can be computed accurately by solving Eq. (3) with the second-order split-operator technique.<sup>24,25</sup>

The effect of damping on the population transfer can be considered by including spontaneous decay into the motion equation (3). For a multi-level SQUID system considered here, the spontaneous decay from a level  $|n\rangle$  can be represented phenomenologically by a damping operator, whose eigenvalue  $\Gamma_n$  in the field-free eigenstate is energy relaxation rate of that level.<sup>26</sup> If the time-dependent wave function is also expanded in the field-free eigenstates, we obtain an equation similar to Eq. (3) with the Hamiltonian  $\tilde{H}$  given by<sup>12,27</sup>

$$\tilde{H}_{nn'}(\tau) = H_{nn'}(\tau) - i\gamma_n \delta_{nn'}/2, \quad (5)$$

where  $\gamma_n \equiv \Gamma_n/\hbar\omega_{LC}$  is reduced energy relaxation rate from the level  $|n\rangle$ . Replacing the Hamiltonian  $H$  in Eq. (3) by  $\tilde{H}$ , we obtain an additional term  $-i\gamma_n c_n/2$  for the level  $|n\rangle$ . Due to this term, the population  $P_n(\tau) = P_n(0)\exp(-\gamma_n\tau)$  decays exponentially at a rate of  $\gamma_n$ .<sup>12,28</sup> This term resulted from the energy relaxation of the level  $|n\rangle$  and thus is the reflection of energy-relaxation-induced decoherence. Because it is proportional to  $c_n$ , the energy-relaxation-induced decoherence can

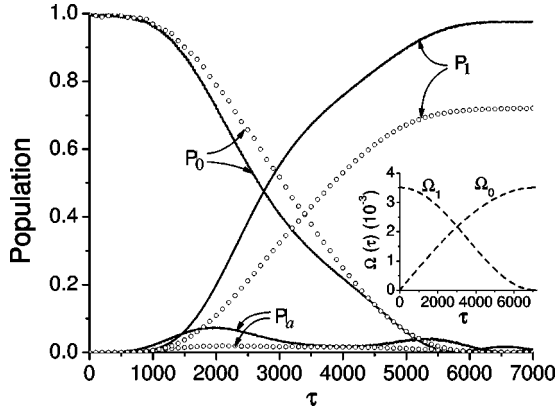


FIG. 2. The same as Fig. 1 but using sine and cosine overlapping microwave pulses. For the sine pulse  $A_0=8 \times 10^{-4}$  and for the cosine pulse  $A_1=5.9 \times 10^{-4}$ . The effective pulse area  $\Omega_{\text{eff}}\tau_l \approx 12.5$ . In the inset, the pulses used are plotted.

be eliminated by keeping the level  $|n\rangle$  unpopulated, i.e., a dark state.

For an ideal  $\Lambda$ -type three-level system without damping, the adiabatic population transfer between the levels  $|0\rangle$  and  $|1\rangle$  through the level  $|a\rangle$  requires<sup>18</sup>

$$\Omega_{\text{eff}}\tau_l \gg 1, \quad (6)$$

where,  $\Omega_{\text{eff}} = \sqrt{\Omega_0^2 + \Omega_1^2}/2$  is effective Rabi flopping frequency and  $\Omega_i \equiv \Omega_{i0}f_i(\tau)$  is the Rabi frequency of the  $|i\rangle \leftrightarrow |a\rangle$  transition with the maximum value  $\Omega_{i0} \equiv m\omega_{LC}|x_{ia}|A_i/\hbar$  (all  $\Omega$ 's are normalized to  $\omega_{LC}$ ). The condition, Eq. (6), shows that a complete transfer could occur if the effective pulse area  $\Omega_{\text{eff}}\tau_l$  is much larger than unity and that the details of each pulse are not important. For a given pulse duration  $\tau_l$ , Eq.(6) can be satisfied by increasing the pulse amplitudes. However, in order to keep the intrinsic errors due to multi-photon processes negligibly small, weak microwave pulses (i.e.,  $\Omega_{i0}/\omega_i \ll 1$ ) must be used. For the weak microwaves, the 3LQ may be approximated by the  $\Lambda$ -type three-level system.<sup>9</sup> Thus the condition, Eq. (6), is expected to be applicable to the 3LQ. Furthermore, although  $\Omega_{\text{eff}}$  could be time-dependent in general, keeping  $\Omega_{\text{eff}}$  time-independent would lead to the shortest pulse duration that satisfies Eq. (6). Without the loss of generality, let  $\Omega_{00} = \Omega_{10} \equiv \Omega_R$ , one has from Eq. (6) for the microwave pulses,

$$A_0|x_{0a}| = A_1|x_{1a}|, \quad f_0^2(\tau) + f_1^2(\tau) = \text{const.} \quad (7)$$

We first examine the simplest case of two completely overlapping rectangular pulses that satisfy Eq. (7). In this case, the pulse shape functions,  $f_0(\tau) = f_1(\tau) = 1$ , and the amplitudes are set to be  $A_0 = 2 \times 10^{-4}$  and  $A_1 = 1.48 \times 10^{-4}$ , respectively, so that  $\Omega_0 = \Omega_1 \ll \omega_{a0}$  and  $\omega_{a1}$ . The lowest 20 levels are taken into account in the calculation. In Fig. 1, we show, by the solid lines, the evolution of populations  $P_0$ ,  $P_1$ , and  $P_a$  obtained by numerically solving Eq. (3) for the 3LQ without damping. For the weak fields considered here, our numerical results are in very good agreement with the analytical predictions of the  $\Lambda$ -type

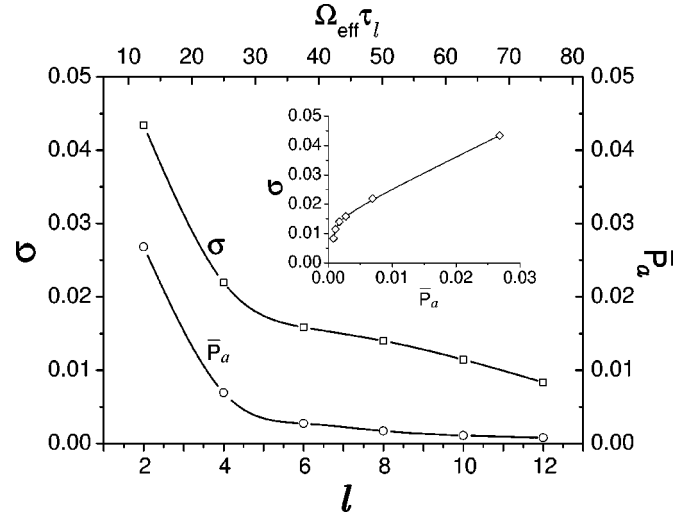


FIG. 3. The  $\sigma$  versus the  $l$  and the  $\bar{P}_a$  versus  $l$  for a 3LQ qubit with  $\gamma_a = 1.24 \times 10^{-4}$ . In the inset,  $\sigma$  is plotted versus  $\bar{P}_a$ .

three-level system:<sup>28</sup> The populations  $P_0$ ,  $P_1$ , and  $P_a$  change periodically with time, and at times  $\tau = 2l\sqrt{2}\pi/\Omega_R$  ( $l=0,1,2,\dots$ , is called the pulse area index hereafter),  $P_0$  reaches unity, while at times  $\tau = (2l+1)\sqrt{2}\pi/\Omega_R$  ( $l=0,1,2,\dots$ ),  $P_1$  reaches unity. Compared with the case of the two sequentially nonoverlapping pulses,<sup>9</sup> the minimum time needed for the bit-flip operation  $\tau_l = \sqrt{2}\pi/\Omega_R$  is about 30% shorter, and, more importantly, the maximum population  $P_a^m (=0.5)$  and average population  $\bar{P}_a [= \tau_l^{-1} \int_0^{\tau_l} P_a(\tau) d\tau]$  of the auxiliary level are much smaller.

To investigate the effect of energy-relaxation-induced decoherence, we perform a similar calculation for the 3LQ above with finite damping by solving Eq. (3) with the Hamiltonian  $\tilde{H}$  given by Eq. (5). The same rectangular pulses are used and the reduced energy relaxation rate is taken to be  $\gamma_a = 1.86 \times 10^{-3}$ , which corresponds to an effective damping resistance  $R = 65 \text{ k}\Omega$  ( $R/R_Q = 10$ ).<sup>29,30</sup> The evolution of populations  $P_0$ ,  $P_1$ , and  $P_a$  are plotted in Fig. 1 with the open circles. At the end of the  $\pi$  pulses,  $P_0 \approx 0.3$  and  $P_1 \approx 0.25$ , which illustrate that the energy-relaxation-induced decoherence is large when the population on the auxiliary level is non-zero for qubits with damping.

Next, by using more sophisticated pulses that satisfy Eq. (7), we show that the population on the auxiliary level can be suppressed in a systematic way. Let us consider two overlapping counterintuitive sine and cosine pulses<sup>14,15</sup> described by  $f_0(\tau) = \sin(\pi\tau/2\tau_l)$  and  $f_1(\tau) = \cos(\pi\tau/2\tau_l)$ . These pulses, which are plotted in the inset of Fig. 2, lead to a time-independent  $\Omega_{\text{eff}}$ . The parameters of the pulses used are the amplitudes of the pulses  $A_0 = 8 \times 10^{-4}$ ,  $A_1 = 5.9 \times 10^{-4}$ , and the duration  $\tau_l = 7120$  which corresponds to the pulse area  $\Omega_{\text{eff}}\tau_l \approx 12.5$  and the pulse area index  $l=2$  [see Eq. (8)]. Suppose that the initial state of the qubit is  $|0\rangle$ , the evolution of populations  $P_0$ ,  $P_1$ , and  $P_a$  calculated from Eq. (3) for the 3LQ without damping is shown in Fig. 2 by the solid lines.

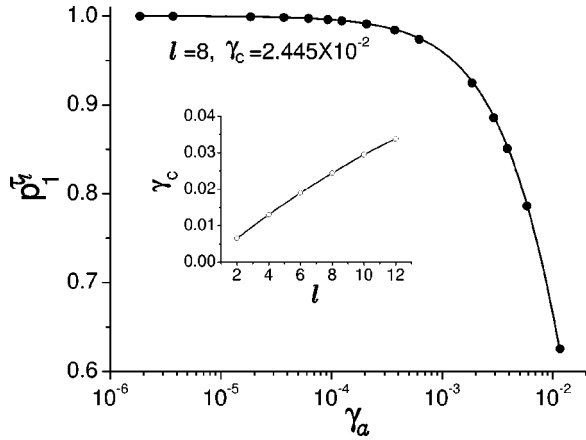


FIG. 4. The  $p_1^7$  versus the  $\gamma_a$ . The pulses are the same as those in Fig. 2 but the effective pulse area  $\Omega_{\text{eff}}\tau_l=50$ . The solid circles and line are the numerical results and exponential fitting. In the inset,  $\gamma_c$  is plotted versus  $l$ .

These results agree qualitatively with the theoretical predictions for the  $\Lambda$ -type three-level systems,<sup>15</sup> for which  $P_1$  reaches the maximum when

$$\Omega_{\text{eff}}\tau_l = 2\pi\sqrt{l^2 - 1/16} \gg 1 \quad (l = 1, 2, \dots). \quad (8)$$

The only substantial difference is that the maximum population on the level  $|a\rangle$  obtained numerically for the 3LQ is greater than the value expected for the  $\Lambda$ -type three-level system,  $P_a^m = 1/4l^2 - 1/16l^4$ . Note that in comparison with the case of rectangular pulses  $\bar{P}_a$  is much smaller in this case. Since the probability of spontaneous decay from the level  $|a\rangle$  is proportional to  $\bar{P}_a\tau_l$  which varies approximately as  $1/\tau_l$ , the error caused by energy relaxation can be made smaller by using longer pulses. However, as the pulse duration becomes longer, other error mechanisms may set in, which imposes additional constraints on the selection of the optimal pulse duration.

To study the influence of  $P_a$  on the population transfer between  $|0\rangle$  and  $|1\rangle$  in the 3LQ with damping, we calculate the evolution of populations  $P_0$ ,  $P_1$ , and  $P_a$  for the SQUID with the same damping  $\gamma_a = 1.86 \times 10^{-3}$  as that used for the rectangular pulses. The results are displayed by the open circles in Fig. 2. Compared to the populations in Fig. 1, the average population of the level  $|a\rangle$  is much smaller. At the end of the pulses,  $P_0 \approx 0$  and  $P_1 \approx 0.7$ , illustrating that the effect of the energy relaxation can be reduced effectively by decreasing  $\bar{P}_a$ .

The energy-relaxation-induced decoherence, which makes the population of the level  $|1\rangle$  at the end of the pulses,  $P_1^7$ , less than unity, can be characterized by the probability of bit-flip error,  $\sigma \equiv 1 - P_1^7$ . Obviously,  $\sigma$  depends on both the effective pulse area  $\Omega_{\text{eff}}\tau_l$  (hence  $\bar{P}_a$ ) and  $\gamma_a$ . For a flux qubit with  $\gamma_a = 1.24 \times 10^{-4}$  (corresponding to  $R \approx 1 \text{ M}\Omega$  and the characteristic time  $T_1 \approx 16 \text{ ns}$ ),  $\sigma$  versus  $l$  and  $\bar{P}_a$  versus  $l$  are shown in Fig. 3, and  $\sigma$  versus  $\bar{P}_a$  is plotted in the inset. From Fig. 3 and the inset, it is clear that  $\sigma$  decreases rapidly

as  $\bar{P}_a$  is reduced. Hence, keeping the level  $|a\rangle$  dark would essentially eliminate the energy-relaxation-induced error. To exclude other possible effects and quantify the causal relationship between  $\sigma$  and  $\gamma_a$ , the normalized population on the level  $|1\rangle$  at the end of the pulses,  $p_1^7(\gamma_a) \equiv P_1^7(\gamma_a)/P_1^7(0)$ , is plotted as a function of  $\gamma_a$  in Fig. 4. The pulse shapes and microwave amplitudes used here are same as those in Fig. 2; the duration is 4 times as long as that in Fig. 2, which corresponds to  $\Omega_{\text{eff}}\tau_l=50$  and  $l=8$ . The decay of  $p_1^7$  with  $\gamma_a$  is described very well by an exponential function  $p_1^7(\gamma_a) = \exp[-\gamma_a/\gamma_c(l)]$ .<sup>14</sup> Here,  $\gamma_c(l)$  is called the *critical energy relaxation rate*—a pulse-duration-dependent characteristic decay rate, which is the *maximum* decay rate allowed to keep the normalized bit-flip error  $\sigma$  less than  $1 - e^{-1}$  when the pulse duration is  $\tau_l$ . Note that the value of  $\gamma_a$  depends on the qubit parameters while the value of  $\gamma_c$  depends on  $\bar{P}_a$  and thus the details of the qubit state manipulation. In general, smaller  $\gamma_a$  and larger  $\gamma_c$  lead to a lower error rate. In particular, for  $\gamma_a \ll \gamma_c$  one has  $\sigma \approx \gamma_a/\gamma_c$ . Therefore,  $\gamma_c$  is one of the most important characteristic parameters of the 3LQ when finite damping is taken into account. The inset of Fig. 4 shows that larger  $l$  leads to larger  $\gamma_c$ . Thus longer pulses are more effective to the reduction of the bit-flip error arising from spontaneous decay.

To demonstrate the advantages of the dark-state approach, let us estimate the bit-flip error of a flux qubit with a realistic damping parameter  $R \approx 65 \text{ M}\Omega$  ( $R/R_Q = 10^4$ ). The energy relaxation rate for such a flux qubit is  $\gamma_a = 1.86 \times 10^{-6}$  (corresponding to  $T_1 \approx 1 \mu\text{s}$ ) at temperature  $T \ll \hbar\omega_{a1}/k_B$ .<sup>29,30</sup> For the three-level bit-flip operation described in Ref. 9 with  $\bar{P}_a \sim 1$ , one has  $\gamma_c \sim \gamma_a$ . In contrast, for the dark-state approach the critical energy relaxation rate increases dramatically to  $\gamma_c \approx 1.9 \times 10^{-2} \approx 10^4 \gamma_a$  for the  $l=6$  pulse sequence, demonstrating the effectiveness of the dark-state approach in reducing the bit-flip error caused by energy relaxation of the excited state.

In summary, by numerical calculation of the population evolution, the effect of the finite damping on the bit-flip operation of the 3LQ is investigated quantitatively. The numerical study uses realistic device parameters and takes into account the multi-level nature of the flux qubits. It is shown that for SQUID flux qubits using a  $\Lambda$ -type three-level as the basic method of coherent state control and manipulation, the bit-flip error originated from energy relaxation of the excited state can be effectively reduced with the use of the dark-state approach in conjunction with the adiabatic transfer of populations. It is also found that when energy relaxation of the excited state is considered, the fidelity of an operation can be characterized by the critical energy relaxation rate  $\gamma_c$ . Quantitatively, for weak damping,  $\gamma_a/\gamma_c \ll 1$ , the probability of bit-flip error from the energy relaxation mechanism is given by  $\sigma \approx \gamma_a/\gamma_c$ . Since the experimentally measured intrinsic damping resistance of Josephson tunnel junctions is greater than  $10^9 \Omega$  at  $T \approx 0.5 \text{ K}$ , the bit-flip error of a flux qubit with such junctions operated by pulses of duration  $\tau_{l=6} \approx 6\sqrt{2}(2\pi/\Omega_R)$  will have  $\sigma < 1.0 \times 10^{-4}$ , a figure that is very attractive for fault-tolerant quantum information processing.

Finally, we should mention that although our investigation is focused on the energy-relaxation-induced decoherence and the effect of dephasing may be different from that of energy relaxation, the decoherence associated with both dephasing and energy relaxation due to a finite population on the auxiliary level can be effectively suppressed by the use of the dark auxiliary level during the operation. Although the dark-state approach can be used to remove the decoherence caused by spontaneous decay from the auxiliary level and to create superposition states, this scheme itself cannot be di-

rectly applied to the gate operation since it works only if the initial state is known.

#### ACKNOWLEDGMENTS

This work was supported by the NSF (EIA-0082499), NSF ITR program (DMR-0325551), and by AFOSR Grant No. F49620-01-1-0439 funded by the Defense University Research Initiative on Nanotechnology (DURINT) program and by the ARDA.

- 
- <sup>1</sup>M. A. Nielsen and I. L. Chuang, *Quantum Computation and Quantum Information* (Cambridge University Press, Cambridge, 2000), Chap. 7.
- <sup>2</sup>Y. Makhlin, G. Schon, and A. Shnirman, *Rev. Mod. Phys.* **73**, 357 (2001).
- <sup>3</sup>J. E. Mooij *et al.*, *Science* **285**, 1036 (1999).
- <sup>4</sup>J. M. Martinis *et al.*, *Phys. Rev. B* **67**, 094510 (2003).
- <sup>5</sup>L. Tian *et al.*, in *Quantum Mesoscopic Phenomena and Mesoscopic Devices in Microelectronics*, edited by I. Kulik and R. Elliatoglu (Kluwer Academic, Dordrecht, 2000), p. 429.
- <sup>6</sup>A. J. Berkley *et al.*, *Phys. Rev. B* **68**, 060502(R) (2003).
- <sup>7</sup>T. Itakura and Y. Tokura, *Phys. Rev. B* **67**, 195320 (2003).
- <sup>8</sup>T. P. Orlando *et al.*, *Phys. Rev. B* **60**, 15 398 (1999).
- <sup>9</sup>Z. Zhou, S.-I. Chu, and S. Han, *Phys. Rev. B* **66**, 054527 (2002).
- <sup>10</sup>C. P. Yang, S.-I. Chu, and S. Han, *Phys. Rev. A* **67**, 042311 (2003).
- <sup>11</sup>M. H. S. Amin *et al.* *Phys. Rev. B* **67**, 100508(R) (2003).
- <sup>12</sup>M. Orszag, *Quantum Optics* (Springer-Verlag, Berlin, 1999), Chap. 2.
- <sup>13</sup>M. Fleischhauer and A. S. Manka, *Phys. Rev. A* **54**, 794 (1996).
- <sup>14</sup>N. V. Vitanov and S. Stenholm, *Phys. Rev. A* **56**, 1463 (1997).
- <sup>15</sup>J. Oreg, F. T. Hioe, and J. H. Eberly, *Phys. Rev. A* **29**, 690 (1984).
- <sup>16</sup>J. R. Kuklinski *et al.*, *Phys. Rev. A* **40**, 6741 (1989).
- <sup>17</sup>A. S. Parkins *et al.*, *Phys. Rev. Lett.* **71**, 3095 (1993).
- <sup>18</sup>C. E. Carroll and F. T. Hioe, *Phys. Rev. A* **42**, 1522 (1990).
- <sup>19</sup>N. V. Vitanov and S. Stenholm, *Phys. Rev. A* **55**, 648 (1997).
- <sup>20</sup>U. Gaubatz *et al.*, *J. Chem. Phys.* **92**, 5363 (1990).
- <sup>21</sup>S. Schiemann *et al.*, *Phys. Rev. Lett.* **71**, 3637 (1993).
- <sup>22</sup>U. Gaubatz *et al.*, *Chem. Phys. Lett.* **149**, 463 (1988).
- <sup>23</sup>P. Marte, P. Zoller, and J. L. Hall, *Phys. Rev. A* **44**, R4118 (1991).
- <sup>24</sup>M. R. Hermann and J. A. Fleck, Jr., *Phys. Rev. A* **38**, 6000 (1988).
- <sup>25</sup>T.-F. Jiang and S.-I. Chu, *Phys. Rev. A* **46**, 7322 (1992).
- <sup>26</sup>T. S. Ho and S.-I. Chu, *Phys. Rev. A* **32**, 377 (1985).
- <sup>27</sup>J. H. Eberly and V. V. Kozlov, *Phys. Rev. Lett.* **88**, 243604 (2002).
- <sup>28</sup>M. O. Scully and M. S. Zubairy, *Quantum Optics* (Cambridge University Press, Cambridge, 1997), Chap. 6.
- <sup>29</sup>A. I. Larkin and Y. N. Ovchinnikov, *Sov. Phys. JETP* **64**, 185 (1986).
- <sup>30</sup>S. Han *et al.*, *Science* **293**, 1457 (2001).